

Title	Enhancing power conversion efficiencies and operational stability of organic light-emitting diodes by increasing carrier injection efficiencies at anode/organic and organic/organic heterojunction interfaces
Author(s)	Matsushima, Toshinori; Murata, Hideyuki
Citation	Journal of Applied Physics, 104(3): 034507-1-034507-4
Issue Date	2008-08-06
Type	Journal Article
Text version	publisher
URL	http://hdl.handle.net/10119/8541
Rights	Copyright 2008 American Institute of Physics. This article may be downloaded for personal use only. Any other use requires prior permission of the author and the American Institute of Physics. The following article appeared in Toshinori Matsushima, Hideyuki Murata, Journal of Applied Physics, 104(3), 034507 (2008) and may be found at http://link.aip.org/link/?JAPIAU/104/034507/1
Description	



Enhancing power conversion efficiencies and operational stability of organic light-emitting diodes by increasing carrier injection efficiencies at anode/organic and organic/organic heterojunction interfaces

Toshinori Matsushima and Hideyuki Murata^{a)}

School of Materials Science, Japan Advanced Institute of Science and Technology, 1-1 Asahidai, Nomi, Ishikawa 923-1292, Japan

(Received 20 March 2008; accepted 5 June 2008; published online 6 August 2008)

We fabricated long-lived multilayer organic light-emitting diodes (OLEDs), in which a 0.75 nm thick hole-injection layer of molybdenum oxide (MoO₃) and a 5 nm thick mixed layer at an organic/organic heterojunction interface were embedded. The use of the MoO₃ layer and of the mixed layer enhanced carrier injection at anode/organic and organic/organic heterojunction interfaces, resulting in a marked decrease in driving voltage and an increase in power conversion efficiency in the OLEDs. We observed about a factor of 9 improvement in the operational lifetime of the OLEDs by using the MoO₃ layer and the mixed layer as well. We assume that the lifetime improvement originates from the suppression of a thermally induced electrochemical degradation process of organic emitting molecules due to the reduction in the probability of the generation of Joule heat. © 2008 American Institute of Physics. [DOI: 10.1063/1.2964113]

I. INTRODUCTION

Recent research on organic light-emitting diodes (OLEDs) composed of small organic molecules, oligomers, and polymers has been intensive due to their advantages of making low-cost, lightweight, flexible, large-area display, and lighting applications possible.^{1,2} Power conversion efficiencies and operational stability of OLEDs are still inferior to those of inorganic LEDs, and they are the limiting factors for expanding the commercial applications of OLEDs. To improve the power conversion efficiency and the stability, a reduction in driving voltage is essential. For this purpose, a hole-injection layer (HIL) has been frequently used between an indium tin oxide (ITO) anode layer and an organic hole-transport layer (HTL) owing to a reduction in the hole-injection barrier height.^{3–12} The organic materials used in the HILs include copper phthalocyanine,^{4,6} starburst amine,^{3,6} and alpha-sexithiophene.⁹ The inorganic materials used in the HILs include vanadium oxide (V₂O₅),⁵ tungsten oxide (WO₃),^{8,11} and molybdenum oxide (MoO₃),^{5,7,10,12} where the thickness of a MoO₃ HIL inserted between the ITO and *N,N'*-diphenyl-*N,N'*-bis(1-naphthyl)-1,1'-biphenyl-4,4'-diamine (α -NPD) was generally greater than 5 nm. We recently found that the 0.75 nm thick MoO₃ HIL leads to the formation of an Ohmic contact at the ITO/MoO₃/ α -NPD interfaces.¹⁰ Since the reduction in hole-injection barrier height improves the stability of OLEDs,^{4,12} the formation of this Ohmic contact not only produces the lowest driving voltage but also may be expected to improve the stability of OLEDs. However, device characteristics of OLEDs with an Ohmic contact for hole injection have never been investigated. In this study, we show that the insertion of the 0.75 nm thick MoO₃ HIL significantly improves both the driving voltage and the operational stability of OLEDs.

To improve the OLED stability, a mixed layer composed of a HTL material of α -NPD, an electron-transport-layer (ETL) material of tris(8-hydroxyquinoline) aluminum (Alq₃), and a highly efficient fluorescent molecule was used as an emitting layer of OLEDs, which are called bulk heterojunction (BHJ) OLEDs.^{13–23} The reason for the improved stability when using the mixed layer was ascribed to a reduction in the number of unstable cationic Alq₃ molecules due to selective hole hopping on α -NPD molecules in the mixed region.^{14,17,20,22}

The disadvantage of constructing BHJ OLEDs using a mixed layer of a HTL material of α -NPD and an emitting ETL material of Alq₃ is an increase in driving voltage when compared to conventional HJ OLEDs.^{13,23} The voltage increase in BHJ OLEDs is probably due to a decrease in the mobilities of electrons and holes in the mixed layer,²⁴ whose thickness was greater than 50 nm. Recently, the use of a very thin mixed layer with a thickness of 5 nm at a HJ interface has been shown to decrease the driving voltage of OLEDs, which are called interface mixed (IM) OLEDs.²⁵ This voltage decrease is attributable to enhanced carrier injection and carrier recombination efficiencies, which may be due to the increased contact of two organic molecules in a thin mixed region. Here, we found that the formation of a 5 nm thick mixed layer of α -NPD and Alq₃ improves both the driving voltage and the stability of OLEDs. By combining the insertion of the 0.75 nm thick MoO₃ HIL and the 5 nm thick IM layer, we demonstrate the lowest driving voltage and the excellent lifetime of the OLEDs based on an α -NPD HTL and an Alq₃ emitting ETL.

II. EXPERIMENTAL

We fabricated four types of OLEDs named (A), (B), (C), and (D) for comparison, whose schematic structures are illustrated in Fig. 1. The HJ device (A) had a conventional

^{a)}Electronic mail: murata-h@jaist.ac.jp.

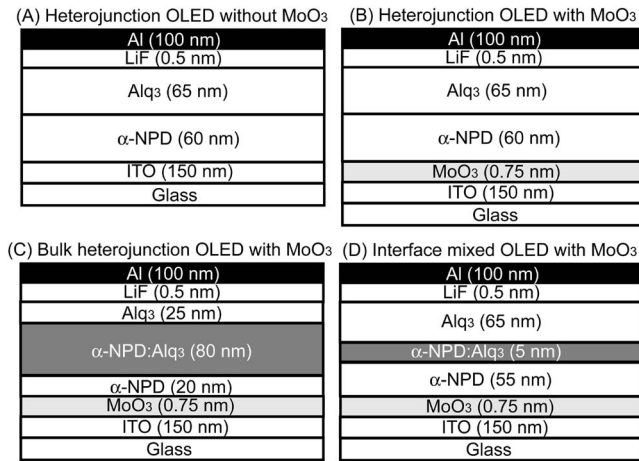


FIG. 1. Schematic structures of OLEDs (A)–(D).

two-layer structure, which was composed of an α -NPD HTL and an Alq₃ emitting ETL. We inserted a 0.75 nm thick HIL of MoO₃ between the ITO and the α -NPD in HJ (B), BHJ (C), and IM (D), which provides Ohmic hole injection at this interface.¹⁰ The thicknesses of the mixed layer of α -NPD and Alq₃ were 80 nm in BHJ (C) and 5 nm in IM (D). The total thickness of the organic layers was 125 nm for all devices.

Glass substrates coated with a 150 nm thick ITO layer with a sheet resistance of 10 Ω /sq (Sanyo Vacuum Industries Co., Ltd.) were used as a hole-injection anode. The cleaning procedure of the substrates included ultrasonication in acetone, detergent, pure water, and isopropanol, and finally UV irradiation in an UV-O₃ chamber. Then, the substrates were placed in a vacuum evaporator, which was evacuated to around 3×10^{-4} Pa. Organic and inorganic layers were successively vacuum deposited on the ITO layer to fabricate the OLED structures shown in Fig. 1. The deposition rates were 0.05 nm/s for MoO₃, 0.1 nm/s for both α -NPD and Alq₃, 0.01 nm/s for LiF, and 0.5 nm/s for Al. The composition ratio of the mixed layers was set at α -NPD/Alq₃=1/1 by mol. The thickness, the deposition rates, and the composition ratio of the layers were controlled using a quartz crystal microbalance. The active area of the devices was defined at 4 mm² by the overlapped area of the ITO and Al layers. High-purity source materials of MoO₃ (6N grade, Mitsuwa Chemicals Co., Ltd), α -NPD (NN60615, Nippon Steel Chemical Co., Ltd.), Alq₃ (NA30516, Nippon Steel Chemical Co., Ltd.), LiF (206–30, Nacalai Tesque Inc.), and Al (AL-011480, Nilaco Co.) were purchased and used as received. The completed devices were transferred to a nitrogen-filled glovebox (O₂ and H₂O levels

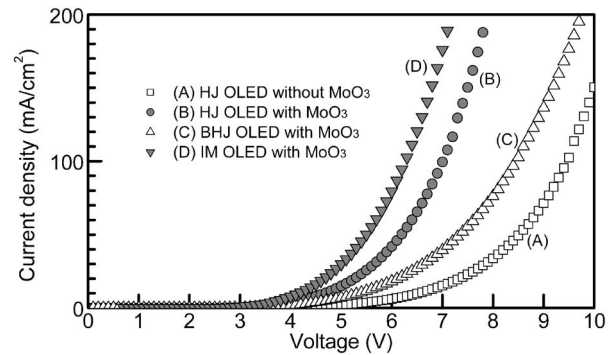


FIG. 2. Current density–voltage characteristics of OLEDs (A)–(D).

less than 2 ppm) without exposing them to ambient air. Then, the devices were encapsulated with a glass cap using an UV curing epoxy resin inside the glovebox. We measured the current density–voltage–external quantum efficiency characteristics of the devices using a semiconductor characterization system (4200, Keithley Instruments Inc.) and an integrating sphere installed with a calibrated silicon photodiode. We measured the current efficiencies and the power conversion efficiencies of the devices based on the luminance values measured with a luminance meter (BM-9, TOPCON Co.) in the direction perpendicular to the substrate surface. It is noteworthy that the efficiencies based on the luminance values may include an effect of an emission pattern from the device surface. To obtain the operational lifetimes and the acceleration coefficients, we continuously operated the devices at a constant dc current density of either 50, 100, 150, or 200 mA/cm². We conducted all measurements at room temperature.

III. RESULTS AND DISCUSSION

The current density–voltage characteristics of the OLEDs (A), (B), (C), and (D) are shown in Fig. 2. The driving voltages of the devices at a current density of 50 mA/cm² were 8.6 ± 0.2 V for HJ (A), 6.1 ± 0.1 V for HJ (B), 7.4 ± 0.2 V for BHJ (C), and 5.6 ± 0.1 V for IM (D) (Table I). The driving voltages decreased by 2.5 V when inserting the 0.75 nm thick MoO₃ HIL between the ITO and the α -NPD [HJ (A) and HJ (B)]. This voltage decrease is attributable to the formation of an Ohmic contact at the ITO/MoO₃/ α -NPD interfaces.¹⁰ We achieved a further decrease in driving voltage, from 6.1 ± 0.1 V [HJ (B)] to 5.6 ± 0.1 V [IM (D)], by inserting the 5 nm thick mixed layer at the HJ interface composed of α -NPD and Alq₃. The

TABLE I. Summary of driving voltages, luminance, current efficiencies, external quantum efficiencies, power conversion efficiencies, and 90% lifetimes of OLEDs (A), (B), (C), and (D), operated at 50 mA/cm².

Sample	Driving voltage (V)	Luminance (cd/m ²)	Current efficiency (cd/A)	External quantum efficiency (%)	Power conversion efficiency (lm/W)	90% lifetime (h)
(A)	8.6 ± 0.2	1800 ± 50	3.60 ± 0.10	1.11 ± 0.01	1.41 ± 0.04	32
(B)	6.1 ± 0.1	1450 ± 40	2.90 ± 0.08	0.94 ± 0.02	1.57 ± 0.05	190
(C)	7.4 ± 0.2	1650 ± 50	3.30 ± 0.10	1.06 ± 0.02	1.50 ± 0.05	231
(D)	5.6 ± 0.1	1440 ± 40	2.88 ± 0.08	0.96 ± 0.02	1.67 ± 0.05	281

enhancement of hole injection from α -NPD to Alq₃ is probably caused by an increased contact of α -NPD and Alq₃ molecules in the mixed layer.²⁵

In contrast, we observed an increase in driving voltage in BHJ (C) (7.4 ± 0.2 V) when compared to HJ (B) (6.1 ± 0.1 V). Since the electron and hole mobilities in the mixed layer of α -NPD and Alq₃ are much lower than the electron mobility of a pure Alq₃ layer and the hole mobility of a pure α -NPD layer,²⁴ the increase in voltage would originate from the lowered mobilities in the 80 nm thick mixed layer. Since the thickness of the mixed layer (5 nm) in IM (D) is much smaller than that of the mixed layer (80 nm) in BHJ (C), we assume that the decrease in carrier mobility is almost negligible in the 5 nm thick mixed layer. Thus, the enhancement of hole injection preferably occurs in the 5 nm thick mixed layer, resulting in the lowest driving voltage observed in IM (D).

Table I summarizes the external quantum efficiencies and power conversion efficiencies of the OLEDs operated at a current density of 50 mA/cm². When the MoO₃ HIL was used, the external quantum efficiencies decreased from $1.11 \pm 0.01\%$ [HJ (A)] to $0.94 \pm 0.02\%$ [HJ (B)]. Since the use of the MoO₃ HIL enhances hole injection from the ITO/MoO₃ anode to the α -NPD, the larger number of holes is expected to reach the carrier recombination zone than electrons. Thus, an excess number of holes in the carrier recombination zone mainly caused the decrease in the external quantum efficiency.²⁶ On the contrary, the external quantum efficiency of BHJ (C) ($1.06 \pm 0.02\%$) was slightly higher than those of HJ (B) ($0.94 \pm 0.02\%$) and IM (D) ($0.96 \pm 0.02\%$). In a separate experiment, we measured the photoluminescence quantum efficiencies of films of pure Alq₃ and a composite of α -NPD/Alq₃ (1/1 by mol) on quartz substrates using an integrating sphere system (C9920-02, Hamamatsu Photonics Co., Ltd.). The photoluminescence quantum efficiencies of an Alq₃ film and a composite film were $18 \pm 1\%$ and $22 \pm 1\%$, respectively. Since the carrier recombination of electrons and holes takes place in the thick mixed layer in BHJ (C), we attribute the increase in external quantum efficiency to the increase in photoluminescence quantum efficiency in the thick mixed layer. The marked decrease in driving voltage in IM (D) overcomes the decrease in the external quantum efficiency. Thus, the power conversion efficiencies increased from 1.41 ± 0.04 [HJ (A)] to 1.67 ± 0.05 lm/W [IM (D)].

The operational stability of the OLEDs was drastically improved by the use of the MoO₃ HIL and the mixed layer of α -NPD and Alq₃. The luminance/initial luminance–time characteristics of (A), (B), (C), and (D) are shown in Fig. 3. The devices were operated at a constant dc current density of 50 mA/cm² at room temperature. The times at which the luminance reaches 90% of the initial luminance (90% lifetimes) were 32 h for HJ (A), 190 h for HJ (B), 231 h for BHJ (C), and 281 h for IM (D). The 90% lifetimes, the initial luminances, and the initial driving voltages are also summarized in Table I.

The 90% lifetimes drastically increased from 32 h [HJ (A)] to 190 h [HJ (B)] by inserting the 0.75 nm thick MoO₃

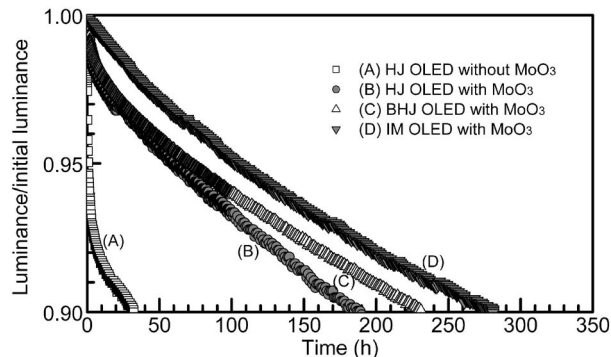


FIG. 3. Luminance/initial luminance–time characteristics (90% lifetimes) of OLEDs (A)–(D), operated at a constant dc current density of 50 mA/cm².

HIL between the ITO and the α -NPD. The luminance of HJ (A) without MoO₃ suddenly decreased at the initial stage of the device operation (Fig. 3). This initial degradation was drastically suppressed by inserting the 0.75 nm thick MoO₃ HIL between the ITO and the α -NPD. This result clearly indicates that the initial degradation of HJ (A) is related to the ITO/ α -NPD interface. The origin of the initial degradation might be attributed to the migration of indium components into the α -NPD HTL (Refs. 27 and 28) and/or a chemical reaction between the α -NPD and hydroxyl groups on the ITO surface.²⁹

The 90% lifetimes further increased from 190 h [HJ (B)] to 231 h [BHJ (C)] and 281 h [IM (D)] by inserting the mixed layer composed of α -NPD and Alq₃. Recently, Aziz *et al.*¹⁴ have proposed that the radical cations of Alq₃ molecules are electrochemically unstable. Since electrochemically decomposed species act as nonradiative recombination centers and/or luminance quenchers in a carrier recombination zone, electroluminescence efficiencies of OLEDs gradually decrease as the amount of decomposed species increases with operational time.^{30–32} This explanation can be consistent with the observed enhancement of the stability from HJ (B) to BHJ (C) but not for IM (D) in which excess cationic species of Alq₃ would be produced. It is well known that operating OLEDs under a higher bias voltage at a higher temperature degrades OLEDs,^{20,33–35} indicating that the device degradation may rapidly proceed under high temperature conditions. From these considerations, decreasing the driving voltages suppresses the generation of Joule heat and may reduce the thermally induced degradation process of the OLEDs.

The relationship between the initial luminance (L_0) and the lifetime (τ) is expressed as the equation

$$L_0^n \tau = \text{const}, \quad (1)$$

where n is the acceleration coefficient.³⁶ To obtain n , we operated (A), (B), (C), and (D) with a constant dc current density of either 50, 100, 150, or 200 mA/cm². Fitting experimental L_0 - τ characteristics with Eq. (1) gave the n values. While HJ (A) without MoO₃ has a smaller $n=1.5$, the other devices yield a higher $n=1.7$. Although the difference in the value of n is still not clearly understood, we are now working to explain it.

We operated IM (D) at a constant dc current density of 150 mA/cm² to obtain its half-lifetime, at which the lumi-

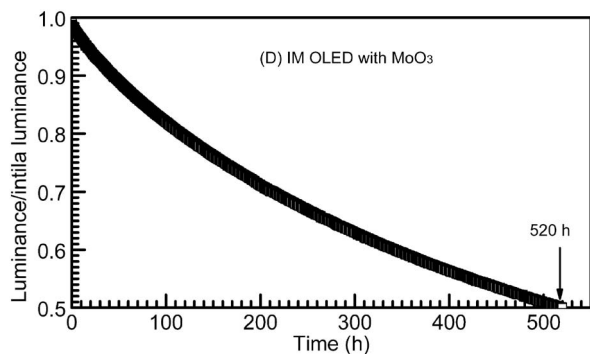


FIG. 4. Luminance/initial luminance–time characteristics (50% lifetimes) of IM (D), operated at a constant dc current density of 150 mA/cm².

nance reaches half of its initial value. The half-lifetime of this device was 520 h for $L_0=4420$ cd/m² (Fig. 4). Using these values, $n=1.7$, and Eq. (1), we calculated the projected half-lifetimes of the OLED at various L_0 to be 6500 h at $L_0=1000$ cd/m², 21 000 h at $L_0=500$ cd/m², 50 000 h at $L_0=300$ cd/m², and 330 000 h at $L_0=100$ cd/m², which lie beyond the half-lifetimes that were previously reported in OLEDs with an Alq₃ emitter. Although we used Alq₃ with a low photoluminescence quantum efficiency of $18 \pm 1\%$ in the present study, doping highly fluorescent or phosphorescent organic molecules into organic host layers of OLEDs will further improve the external quantum efficiency and the operational stability.³⁷

IV. CONCLUSIONS

We have investigated the effect of the insertion of an ultrathin 0.75 nm thick HIL of MoO₃ between an ITO and an α -NPD and of a 5 nm thick mixed layer between an α -NPD and an Alq₃ on the performance of OLEDs. We demonstrated that the use of the thin MoO₃ layer drastically decreases the driving voltage and prevents OLED degradation at an ITO/ α -NPD interface. We showed that the insertion of the thin mixed layer reduces the driving voltage and enhances the stability of the OLED as well. The decrease in driving voltage may reduce the probability of the generation of Joule heat and a thermally induced degradation process in OLEDs.

ACKNOWLEDGMENTS

We thank the New Energy and Industrial Technology Development Organization (NEDO) of Japan for financial support of this work.

- ¹S. R. Forrest, *Nature (London)* **428**, 911 (2004).
- ²N. Koch, *ChemPhysChem* **8**, 1438 (2007).
- ³Y. Shirota, Y. Kuwabara, H. Inada, T. Wakimoto, H. Nakada, Y. Yonemoto, S. Kawami, and K. Imai, *Appl. Phys. Lett.* **65**, 807 (1994).
- ⁴S. A. Van Slyke, C. H. Chen, and C. W. Tang, *Appl. Phys. Lett.* **69**, 2160 (1996).
- ⁵S. Tokito, K. Noda, and Y. Taga, *J. Phys. D* **29**, 2750 (1996).
- ⁶S.-F. Chen and C.-W. Wang, *Appl. Phys. Lett.* **85**, 765 (2004).
- ⁷T. Miyashita, S. Naka, H. Okada, and H. Onnagawa, *Jpn. J. Appl. Phys., Part 1* **44**, 3682 (2005).
- ⁸J. Li, M. Yahiro, K. Ishida, H. Yamada, and K. Matsushige, *Synth. Met.* **151**, 141 (2005).
- ⁹T. Matsushima and C. Adachi, *Appl. Phys. Lett.* **89**, 253506 (2006).
- ¹⁰T. Matsushima, Y. Kinoshita, and H. Murata, *Appl. Phys. Lett.* **91**, 253504 (2007).
- ¹¹J. Meyer, S. Hamwi, T. Bülow, H.-H. Johannes, T. Riedl, and W. Kowalsky, *Appl. Phys. Lett.* **91**, 113506 (2007).
- ¹²H. You, Y. Dai, Z. Zhang, and D. Ma, *J. Appl. Phys.* **101**, 026105 (2007).
- ¹³Z. D. Popovic, H. Aziz, C. P. Tripp, N.-X. Hu, A.-M. Hor, and G. Hu, *Proc. SPIE* **3476**, 68 (1998).
- ¹⁴H. Aziz, Z. D. Popovic, N.-X. Hu, A.-M. Hor, and G. Xu, *Sciences (N.Y.)* **283**, 1900 (1999).
- ¹⁵V.-E. Choong, S. Shi, J. Curless, C.-L. Shieh, H.-C. Lee, F. So, J. Shen, and J. Yang, *Appl. Phys. Lett.* **75**, 172 (1999).
- ¹⁶J. Curless, S. Rogers, M. Kim, M. Lent, S. Shi, V.-E. Choong, C. Briscoe, and F. So, *Synth. Met.* **107**, 53 (1999).
- ¹⁷V.-E. Choong, J. Shen, J. Curless, S. Shi, J. Yang, and F. So, *J. Phys. D* **33**, 760 (2000).
- ¹⁸A. B. Chwang, R. C. Kwong, and J. J. Brown, *Appl. Phys. Lett.* **80**, 725 (2002).
- ¹⁹D. Ma, C. S. Lee, S. T. Lee, and L. S. Hung, *Appl. Phys. Lett.* **80**, 3641 (2002).
- ²⁰H. Aziz, Z. D. Popovic, and N.-X. Hu, *Appl. Phys. Lett.* **81**, 370 (2002).
- ²¹Y. Shao and Y. Yang, *Appl. Phys. Lett.* **83**, 2453 (2003).
- ²²G. Vamvounis, H. Aziz, N.-X. Hu, and Z. D. Popovic, *Synth. Met.* **143**, 69 (2004).
- ²³M. Nakahara, M. Minagawa, T. Oyamada, T. Tadokoro, H. Sasabe, and C. Adachi, *Jpn. J. Appl. Phys., Part 2* **46**, L636 (2007).
- ²⁴S.-W. Liu and J.-K. Wang, *Proc. SPIE* **6333**, 63331R (2006).
- ²⁵T. Matsushima and C. Adachi, *Jpn. J. Appl. Phys., Part 2* **46**, L861 (2007).
- ²⁶T. Tsutsui, *Mater. Res. Bull.* **22**, 39 (1997).
- ²⁷A. R. Schlattmann, D. W. Floet, A. Hilberer, F. Garten, P. J. M. Smulders, T. M. Klapwijk, and G. Hadziioannou, *Appl. Phys. Lett.* **69**, 1764 (1996).
- ²⁸S. T. Lee, Z. Q. Gao, and L. S. Hung, *Appl. Phys. Lett.* **75**, 1404 (1999).
- ²⁹K. Akedo, A. Miura, K. Noda, and H. Fujikawa, *Proceedings of the 13th International Display Workshops, 2006* (unpublished), p. 465.
- ³⁰J. C. Scott, J. H. Kaufman, P. J. Brock, R. DiPietro, J. Salem, and J. A. Goitia, *J. Appl. Phys.* **79**, 2745 (1996).
- ³¹D. Y. Kondakov, W. C. Lenhart, and W. F. Nichols, *J. Appl. Phys.* **101**, 024512 (2007).
- ³²Y. Luo, H. Aziz, Z. D. Popovic, and G. Xu, *J. Appl. Phys.* **101**, 034510 (2007).
- ³³I. D. Parker, Y. Cao, and C. Y. Yang, *J. Appl. Phys.* **85**, 2441 (1999).
- ³⁴H. Murata, C. D. Merritt, H. Inada, Y. Shirota, and Z. H. Kafafi, *Appl. Phys. Lett.* **75**, 3252 (1999).
- ³⁵M. Ishii and Y. Taga, *Appl. Phys. Lett.* **80**, 3430 (2002).
- ³⁶C. Féry, B. Racine, D. Vaufray, H. Doyeux, and S. Cinà, *Appl. Phys. Lett.* **87**, 213502 (2005).
- ³⁷C. W. Tang, S. A. VanSlyke, and C. H. Chen, *J. Appl. Phys.* **65**, 3610 (1989).